Dynamic Performance Assessment: Grazing and Related Phenomena

Vaibhav Donde, *Member, IEEE,* and Ian A. Hiskens, *Senior Member, IEEE*

***Abstract*—Performance specifications place restrictions on the dynamic response of many systems, including power systems. Quantitative assessment of performance requires knowledge of the bounding conditions under which specifications are only just satisfied. In many cases, this limiting behavior can be related to grazing phenomena, where the system trajectory makes tangential contact with a performance constraint. Other limiting behavior can be related to time-driven event triggering. In all cases, pivotal limiting conditions can be formulated as boundary value problems. Numerical shooting methods provide efficient solution of such problems. Dynamic performance assessment is illustrated in the paper using examples drawn from protection operation, transient voltage overshoot, and induction motor stalling.**

***Index Terms*—Boundary value problems, dynamic performance assessment, grazing phenomena, nonlinear nonsmooth system dynamics, shooting methods.**

I. Introduction

POWER system dynamic behavior is subject to performance constraints that seek to ensure appropriate post-disturbance response. Such constraints (bounds) are designed to limit transient excursions. Otherwise excessive swings may trigger protection relays, outaging items of equipment, and possibly leading to cascading system failure [1]. Bounding cases, where the system trajectory just encounters a performance constraint, separate regions of desirable and undesirable behavior. Knowledge of the conditions associated with such bounding cases enables assessment of system vulnerability.

Consider for example a disturbance that causes the system trajectory to pass close to (but not encounter) a protection triggering characteristic [2], [3]. Fig. 1 shows the impedance plane view of distance protection operating characteristics, along with typical system responses. For a particular loading level, the system may follow the path from a_1 (pre-fault stable equilibrium), to $b_1 - c_1$ (fault-on), to d_1 and beyond (post-fault). As the post-fault trajectory does not encounter the relay operating characteristic, protection does not operate, no equipment is tripped, and the system recovers. However, it requires only a small increase in load for protection to operate (trajectory $a_2 - b_2 - c_2$). At this slightly higher loading level, the post-fault trajectory encounters the impedance circle and tripping may occur. (The consequences of such tripping are not shown in the figure.)

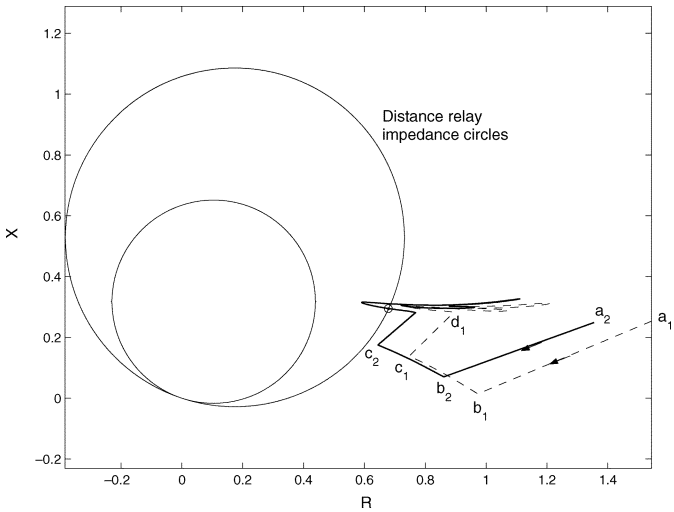

Fig. 1. Power system trajectories in the impedance plane of a distance relay.

Somewhere between the two loading levels of Fig. 1, the trajectory just touches (*grazes*) the protection operating characteristic. Under those conditions, the system becomes vulnerable to protection operation. Such situations are important in the assessment of dynamic performance. It is shown in the paper that grazing points can be formulated as a boundary value problem. Solution using a process that couples Newton's method with numerical integration, known as a shooting method [4], gives the parameter values that induce such grazing phenomena.

Continuing this illustration, typically zone 2 protection, corresponding to the outer circle of Fig. 1, does not trip instantaneously. Rather, the trajectory must remain inside the circle for a pre-specified period for tripping to occur. The paper shows that such *time-difference* event triggers[1] can also be formulated as boundary value problems.

Fig. 2 enables further explanation of grazing concepts. For a certain value of parameter θ_{hit}, the system trajectory encounters a performance constraint (possibly a protection operating characteristic) at a point $x_{\rm hit}$. An event occurs, and the trajectory continues accordingly. For a small change in parameter value, to $\theta_{\rm miss}$, the trajectory misses (at least locally) the constraint and subsequently exhibits a completely different form of response. At a parameter value θ_g, lying between $\theta_{\rm hit}$ and $\theta_{\rm miss}$, the trajectory tangentially encounters (grazes) the constraint. Behavior beyond the grazing point x_g is generally unpredictable. Without further knowledge of the system, it is impossible to determine

Manuscript received November 8, 2004; revised March 21, 2005. This work was supported by the National Science Foundation under Grant ECS-0332777. Paper no. TPWRS–00588–2004.

V. Donde is with the Lawrence Berkeley National Laboratory, Berkeley, CA 94720 USA (e-mail: VDonde@lbl.gov).

I. A. Hiskens is with the University of Wisconsin, Madison, WI 53706 USA (e-mail: hiskens@engr.wisc.edu).

Digital Object Identifier 10.1109/TPWRS.2005.856990

[1]The contrast is with instantaneous event triggers that are associated with grazing.

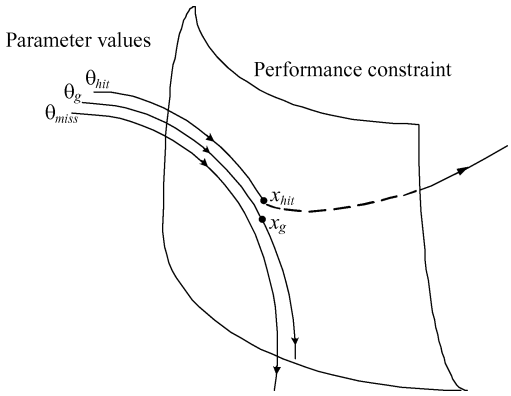

Fig. 2. Grazing phenomenon.

whether or not an event triggers. This bounding case is closely related to *grazing bifurcations* [5]–[7], with θ_g referring to the pivotal value of the bifurcation parameter. The bifurcation interpretation is more appropriate for periodic behavior though. In power systems, grazing is generally a transient phenomenon, so it is not strictly a bifurcation.

Vulnerability to event triggering (and hence some form of undesirable behavior) can be assessed by comparing given (nominal) parameter values with values that induce grazing. If the actual and grazing values differ by a sufficient margin, taking account of parameter and model uncertainty, then appropriate dynamic performance is guaranteed. Crucial to this assessment is the ability to determine grazing values.

The paper is organized as follows. Section II presents a modeling formulation that takes account of the hybrid nature of power system dynamics. Trajectory sensitivity concepts are introduced. Conditions governing grazing phenomena are developed in Section III. Illustrations based on protection and transient voltage overshoot are provided. Section IV discusses time-difference events, with illustrations drawn from protection and induction motor stalling. Conclusions are provided in Section V.

II. Model

A. Hybrid System Representation

In response to large disturbances, power systems typically exhibit periods of smooth behavior, interspersed with discrete events. Smooth behavior is driven by devices such as generators that are well described analytically by differential-algebraic models. Discrete events, arising for example from operation of protection devices or enforcement of controller hard limits, are not so easy to describe analytically. Systems that exhibit intrinsic interactions between continuous dynamics and discrete events have become known generically as *hybrid systems* [8], [9] or *piecewise smooth dynamical systems* [10].

Numerous formal models exist for rigorously describing hybrid system dynamics. Examples include petri nets [11] and hybrid automata [8]. However, those representations are not immediately amenable to numerical implementation. A useful, nonrestrictive model formulation should be

- capable of capturing the full range of continuous/discrete hybrid system dynamics;
- computationally efficient;
- consistent with the development of shooting methods.

It is shown in [12] and [13] that these specifications can be met completely by a model that consists of a set of differential-algebraic equations, adapted to incorporate impulsive (state reset) action and switching of the algebraic equations. This *DA Impulsive Switched* (DAIS) model has its genesis in the familiar DAE model

$$\dot{x} = f(x, y) \tag{1}$$

$$0 = g(x, y) \tag{2}$$

where $x \in \mathbb{R}^n$ are dynamic states, $y \in \mathbb{R}^m$ are algebraic states, $f : \mathbb{R}^{n+m} \to \mathbb{R}^n$, and $g : \mathbb{R}^{n+m} \to \mathbb{R}^m$.

Events such as line tripping can be incorporated into the model by allowing algebraic equations (2) to switch between sets of equations that describe the different system conditions. Other events, such as transformer tapping or protection timer resetting [14], are best modeled by impulsive action that introduces discrete jumps into the x-states. Such behavior has the form of a reset equation

$$x^+ = h(x^-, y^-) \tag{3}$$

where $h : \mathbb{R}^{n+m} \to \mathbb{R}^n$. The notation x^+ denotes the value of x just after the reset event, while x^- and y^- refer to the values of x and y just prior to the event.

Full details of the DAIS model can be found in [12] and [15]. It should be emphasized that the DAIS model is nothing more than a formalization of simulation models that are used for practical power system simulation. The formalization, however, allows trajectory sensitivities to be clearly defined [13].

Dynamic behavior, generated by simulation, can be described analytically by the *flow*

$$x(t) = \phi(x_0, t) \tag{4}$$

together with algebraic constraints

$$g(\phi(x_0, t), y(t)) = 0 \tag{5}$$

where g takes account of switching events. Initial conditions imply

$$\phi(x_0, t_0) = x_0. \tag{6}$$

A compact development of boundary value problems results from incorporating parameters $p \in \mathbb{R}^\ell$ into the dynamic states x. (Numerical implementation is also simplified.) This is achieved by introducing trivial differential equations

$$\dot{p} = 0 \tag{7}$$

into (1) and results in the natural partitioning

$$x = \begin{bmatrix} \underline{x} \\ p \end{bmatrix}, \quad f = \begin{bmatrix} \underline{f} \\ 0 \end{bmatrix}, \quad h = \begin{bmatrix} \underline{h} \\ p \end{bmatrix} \tag{8}$$

where $\underline{x}$ are the true dynamic states, and p are parameters.

B. Trajectory Sensitivities

Shooting method algorithms, which form the basis for solving boundary value problems, require the sensitivity of a trajectory (flow) to perturbations in parameters and/or initial conditions

[4]. To obtain the sensitivity of the flow ϕ to initial conditions x_0, the Taylor series expansion of (4) is formed. Neglecting higher order terms gives

$$\Delta x(t) = \frac{\partial \phi(t)}{\partial x_0} \Delta x_0 \equiv \Phi(x_0, t) \Delta x_0 \tag{9}$$

where Φ is the *sensitivity transition matrix*, or *trajectory sensitivities*, associated with the x flow [16]. Equation (9) describes the change $\Delta x(t)$ in a trajectory, at time t along the trajectory, for a given (small) change in initial conditions $\Delta x_0 = \left[\Delta \underline{x}_0^T \ \Delta p^T\right]^T$.

Space limitations preclude the inclusion of the variational equations describing the evolution of Φ. Full details are given in [12] and [13]. It should be emphasized that Φ does not require smoothness of the underlying flow ϕ. Trajectory sensitivities are well defined for the nonsmooth and/or discontinuous flows associated with realistic power systems.

Furthermore, the computational burden of generating Φ is minimal. It is shown in [13], [17], and [18] that when an implicit numerical integration technique such as trapezoidal integration is used, trajectory sensitivities can be obtained as a by-product of computing the underlying trajectory.

III. Grazing

A. Context

Grazing phenomena have been widely investigated recently, particularly with reference to periodic systems [5], [19], [20]. In that context, grazing is closely related to border-collision bifurcations [6], [21], [22], which are also known as C-bifurcations [23]. Transient grazing was considered in [24] and [25], where switching-time bifurcations were analyzed. These previous investigations focused largely on classifying the (local) consequences of bifurcations through normal form analysis, particularly for periodic systems. Computation of actual grazing points has received less attention, with *ad hoc* approaches prevailing. This paper addresses that deficiency by establishing a shooting method that is applicable for general nonlinear hybrid systems, such as power systems.

B. Mathematical Description

Grazing is characterized by a trajectory (flow) of the system touching a performance constraint (for example a protection triggering hypersurface) tangentially. Let that target hypersurface be described by

$$b(x, y) = 0 \tag{10}$$

where $b : \mathbb{R}^{n+m} \to \mathbb{R}$. Vectors that are normal to b are given by $\nabla b = [\partial b/\partial x \ \partial b/\partial y]^T \equiv [b_x \ b_y]^T$, and the tangent hyperplane is spanned by vectors $\left[u^T \ v^T\right]^T$ that satisfy

$$[b_x \ b_y] \begin{bmatrix} u \\ v \end{bmatrix} = 0. \tag{11}$$

The vector $\left[\dot{x}^T \ \dot{y}^T\right]^T$ is directed tangentially along the flow. To achieve tangential contact between the flow and the target hypersurface, it must satisfy (11) at a grazing point. Furthermore, differentiating (2) and substituting (1) gives

$$0 = \frac{\partial g}{\partial x}\dot{x} + \frac{\partial g}{\partial y}\dot{y} \tag{12}$$

$$\Rightarrow 0 = g_x f(x, y) + g_y v \tag{13}$$

where for notational convenience v replaces $\dot{y}$.

A single degree of freedom is available for varying parameters to find a grazing point. Recall from (8) that parameters p are incorporated into the initial conditions x_0. Therefore, the single degree of freedom can be achieved by parameterization $x_0(\theta)$, where θ is a scalar.

Grazing points are described by combining together the flow definition (4) (appropriately parameterized by θ), algebraic equations (2), target hypersurface (10), and tangency conditions (11), (13) to give

$$F_{g1}(x_g, \theta, t_g) := \phi(x_0(\theta), t_g) - x_g = 0 \tag{14}$$

$$F_{g2}(x_g, y_g) := g(x_g, y_g) = 0 \tag{15}$$

$$F_{g3}(x_g, y_g) := b(x_g, y_g) = 0 \tag{16}$$

$$F_{g4}(x_g, y_g, v) := \begin{bmatrix} b_x & b_y \\ g_x & g_y \end{bmatrix} \begin{bmatrix} f(x_g, y_g) \\ v \end{bmatrix} = 0 \tag{17}$$

where the partial derivatives in (17) are evaluated at the grazing point x_g, y_g. The grazing point occurs at time t_g along the trajectory. This set of equations may be written compactly as

$$F_g(x_g, y_g, \theta, t_g, v) = F_g(z) = 0 \tag{18}$$

where $z = \left[x_g^T \ y_g^T \ \theta \ t_g \ v^T\right]^T$, and $F_g : \mathbb{R}^{n+2m+2} \to \mathbb{R}^{n+2m+2}$. Solution of (18) can be achieved using a shooting method, as discussed in the following section.

C. Shooting Method

1) Algorithm: Numerical solution of (18) using Newton's method amounts to iterating on the standard update formula

$$z^{k+1} = z^k - \left(DF_g(z^k)\right)^{-1} F_g\left(z^k\right) \tag{19}$$

where DF_g is the Jacobian matrix given by (20), shown at the bottom of the next page, with

$$\hat{f} = \begin{bmatrix} f & & & \\ & f & & \\ & & \ddots & \\ & & & f \end{bmatrix}, \quad \hat{v} = \begin{bmatrix} v & & & \\ & v & & \\ & & \ddots & \\ & & & v \end{bmatrix} \tag{21}$$

$$g_{xx} = \begin{bmatrix} \frac{\partial^2 g_1}{\partial x^2} \\ \frac{\partial^2 g_2}{\partial x^2} \\ \vdots \\ \frac{\partial^2 g_m}{\partial x^2} \end{bmatrix}, \quad g_{yx} = \begin{bmatrix} \frac{\partial^2 g_1}{\partial y \partial x} \\ \frac{\partial^2 g_2}{\partial y \partial x} \\ \vdots \\ \frac{\partial^2 g_m}{\partial y \partial x} \end{bmatrix} \tag{22}$$

$$g_{yy} = \begin{bmatrix} \frac{\partial^2 g_1}{\partial y^2} \\ \frac{\partial^2 g_2}{\partial y^2} \\ \vdots \\ \frac{\partial^2 g_m}{\partial y^2} \end{bmatrix}, \quad g_{xy} = \begin{bmatrix} \frac{\partial^2 g_1}{\partial x \partial y} \\ \frac{\partial^2 g_2}{\partial x \partial y} \\ \vdots \\ \frac{\partial^2 g_m}{\partial x \partial y} \end{bmatrix}. \tag{23}$$

The matrices g_{xx}, g_{yx}, g_{xy}, and g_{yy} are usually extremely sparse. It has been found that often the error introduced into DF_g by ignoring them has a negligible effect on convergence. However, situations can arise where these terms are vital for reliable convergence. This is the case, for example, when the trajectory has multiple turning points (peaks and troughs) in the vicinity of the target hypersurface. Two approaches have been used to obtain the second derivative terms.

1) *Numerical differencing.* Many simulators provide direct computation of g_x and g_y, as these quantities are required for implicit numerical integration. Numerical differencing of g_x and g_y is straightforward but not particularly efficient for high dimensional systems.
2) *Direct computation.* By utilizing an object oriented modeling structure [15], second derivative terms occur only within components. There are no terms introduced by inter-component dependencies. Explicit formulae for second derivative terms can be established for each separate component model. The sparse matrices can then be efficiently constructed.

Care must be taken in evaluating the terms of (14)–(17) and (20) that relate to trajectory solution. The flow term $\phi\left(x_0\left(\theta^k\right), t_g^k\right)$ in (14) evaluates, via numerical integration, to the value of x at time t_g^k along the trajectory that has initial value $x_0\left(\theta^k\right)$. Likewise, the terms Φ and f in the first row of DF_g should also be evaluated at time t_g^k along that trajectory. All other terms in DF_g should be evaluated at x_g^k, y_g^k.

2) Initialization of Variables: As with all iterative procedures, solution of (19) requires a reasonable initial guess z^0. In terms of the original system variables, initial (approximate) grazing point values of $x_g^0, y_g^0, \theta^0, t_g^0$, and v^0 are required. These can be obtained from regular simulation.

Referring to Fig. 2, parameter values that are near the pivotal value result in trajectories that either encounter the target hypersurface or just miss the hypersurface. The trajectory induced by parameter θ^0 should be monitored for the following:

1) a point where $b(x,y) = 0$, i.e., an intersection with the target hypersurface; or
2) an appropriate local minimum of $b(x,y)$, i.e., a point where the trajectory passes close by the target hypersurface. Such a point is given by $db/dt = b_x\dot{x} + b_y\dot{y} = 0$. It follows from the discussion underlying the tangency condition (17) that

$$\begin{bmatrix} b_x & b_y \\ g_x & g_y \end{bmatrix} \begin{bmatrix} f(x,y) \\ v \end{bmatrix} = \begin{bmatrix} \frac{db}{dt} \\ 0 \end{bmatrix}. \tag{24}$$

This can be solved sparsely for db/dt as the trajectory is traversed. (In fact, if an implicit numerical integration technique is used, the factors of g_y are already available from computing the trajectory point.) A zero crossing indicates the desired initialization point.

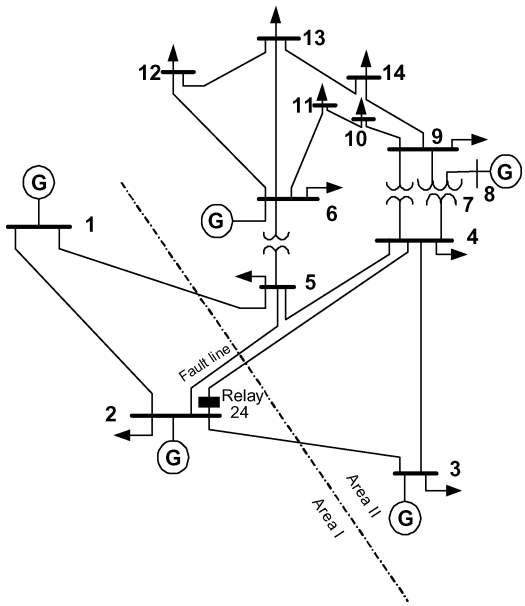

Fig. 3. Modified IEEE 14-bus system.

In both cases, the identified point directly provides initial values for x_g^0, y_g^0, and t_g^0. The corresponding value of v^0 is given as a by-product of (24) in case 2) or by sparsely solving

$$g_y v^0 = -g_x f\left(x_g^0, y_g^0\right)$$

for case 1).

3) Computational Effort: The computational effort involved in solving (19) is primarily associated with repeated simulations. As previously mentioned, the trajectory sensitivities required in the construction of the Jacobian (20) can be computed as a by-product of simulation. Even though (20) has high dimension, it is extremely sparse and can be efficiently factored.

Adoption of a trial-and-error strategy for solving (18) would save formation and factorization of (20). However, the convergence properties of such algorithms are generally inferior to Newton's method. The computational cost of extra simulations far exceeds that of building and factoring (20).

D. Example: Protection

The IEEE 14-bus system of Fig. 3 will be used to illustrate a grazing situation that involves the distance protection on transmission line 2–4 at bus 2. Basic network data for this system can be found in [26], with complete generator/AVR/PSS data given in [27]. To achieve the desired illustration, the impedances

$$DF_g = \begin{bmatrix} -I & 0 & \Phi\frac{dx_0}{d\theta} & f & 0 \\ g_x & g_y & 0 & 0 & 0 \\ b_x & b_y & 0 & 0 & 0 \\ f^T b_{xx} + b_x f_x + v^T b_{yx} & f^T b_{xy} + b_x f_y + v^T b_{yy} & 0 & 0 & b_y \\ \hat{f}^T g_{xx} + g_x f_x + \hat{v}^T g_{yx} & \hat{f}^T g_{xy} + g_x f_y + \hat{v}^T g_{yy} & 0 & 0 & g_y \end{bmatrix} \tag{20}$$

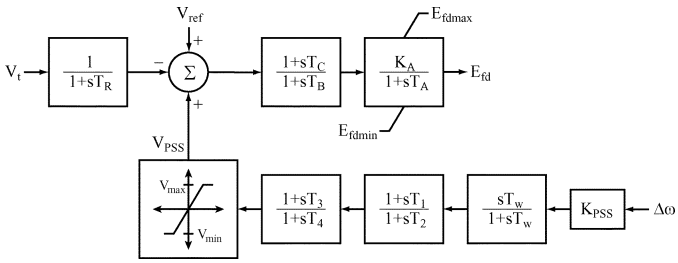

Fig. 4. AVR/PSS standard models AC4A and PSS1A.

TABLE I
SHOOTING METHOD CONVERGENCE, PROTECTION GRAZING

Iter	Grazing values	
	ΔP_L at bus 4	Time, t_g (sec)
0	00.0%	0.39
1	33.8%	0.38
2	49.5%	0.40
3	50.5%	0.41
4	50.7%	0.41

of lines 1–5, 2–5, 2–4, and 2–3 have been increased beyond their standard values, so as to force the system to behave as two areas. This induces post-fault oscillations that lie near the zone 2 impedance circle of relay 24.

A three-phase fault was applied at the midpoint of line 2–5 and was cleared by removing the line from service at 0.1 s after fault inception. Relay 24 monitors the apparent impedance seen looking along line 2–4. For now it will be assumed that the relay issues an instantaneous trip signal if that apparent impedance passes into the operating circle. As mentioned earlier, actual zone 2 behavior involves a time delay before tripping. That situation is considered in Section IV. Grazing is still a very useful concept though, as it provides an indication of system vulnerability.

A sixth-order model (two axes, with two windings on each axis) [28] was used for each machine. All AVR/PSSs were represented by the standard models AC4A and PSS1A [29] shown in Fig. 4. A static voltage-dependent representation was used for all loads.

Referring back to Fig. 1, those two trajectories corresponded to different values of real power demand at bus 4. (The difference in load was matched by adjustment of the output of generator 2.) The aim is to determine the increase in bus 4 load that results in the apparent impedance trajectory grazing the protection operating characteristic. It is shown in [3] that this target hypersurface has the form

$$b(x,y) \equiv \left| \frac{2v_i \angle \alpha_i}{v_i \angle \alpha_i - v_k \angle \alpha_k} - \beta \right| - \beta = 0 \qquad (25)$$

where bus voltage magnitudes v_i and angles α_i are algebraic states and $\beta = 1.2$ for zone 2 relays.

The shooting method of Section III-C was used to find the desired grazing point. Convergence was obtained in four iterations, with progress reported in Table I. An increase in bus 4 load of 50.7%, from its original value of $(96.7 + j33.83)$ MVA, resulted in grazing. The initial and grazing trajectories are shown in Fig. 5.

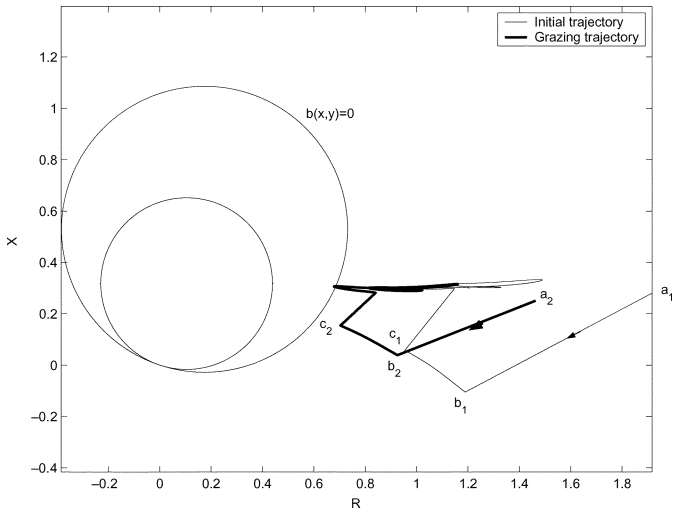

Fig. 5. Impedance trajectories, initial, and grazing conditions.

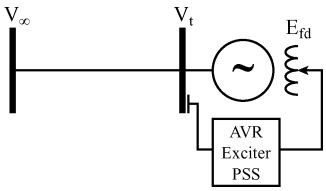

Fig. 6. Single machine infinite bus system.

This example is revisited later, for the case where a tripping time delay is considered.

E. Example: Transient Voltage Overshoot

Further illustration of grazing is provided by considering transient excursions of generator terminal voltage. The single machine infinite bus power system of Fig. 6 forms the basis for this example. The generator was accurately represented by a sixth-order machine model, and the generator excitation system was modeled according to Fig. 4. Note that the output limits on the field voltage E_{fd} are anti-wind-up limits, while the limits on the stabilizer output $V_{\rm PSS}$ are clipping limits [30]. Therefore, even though this example utilizes a simple network structure, it exhibits nonlinear, nonsmooth, hybrid system behavior. Larger systems are no more challenging. A single phase fault was applied at the generator terminal bus at 0.05 s. The fault was cleared, without line tripping, at 0.28 s.

Generators are susceptible to over-voltage protection operation if their terminal voltage rises too high. This may occur during transients following a large disturbance. The field voltage maximum limit $E_{fd\max}$ has a large influence on transient over-voltages. This example considers the maximum value of $E_{fd\max}$ that ensures the initial voltage overshoot does not rise above a specified value of 1.2 p.u. The target hypersurface in this case is therefore $b(x,y) \equiv V_t - 1.2 = 0$.

Results of the iterative solution process are given in Table II and presented graphically in Figs. 7 and 8. Convergence of the shooting method was achieved in four iterations. This is an encouraging result, as an onerous test condition was chosen. Referring to Fig. 7, it can be seen that the original voltage trajectory is quite flat over the first extended peak. The grazing formulation

TABLE II
SHOOTING METHOD CONVERGENCE, VOLTAGE CONSTRAINT GRAZING

Iter	Grazing values	
	Param, $E_{fd\max}$	Time, t_g (sec)
0	5.80	1.14
1	3.16	1.28
2	4.37	1.19
3	4.72	1.20
4	4.78	1.21

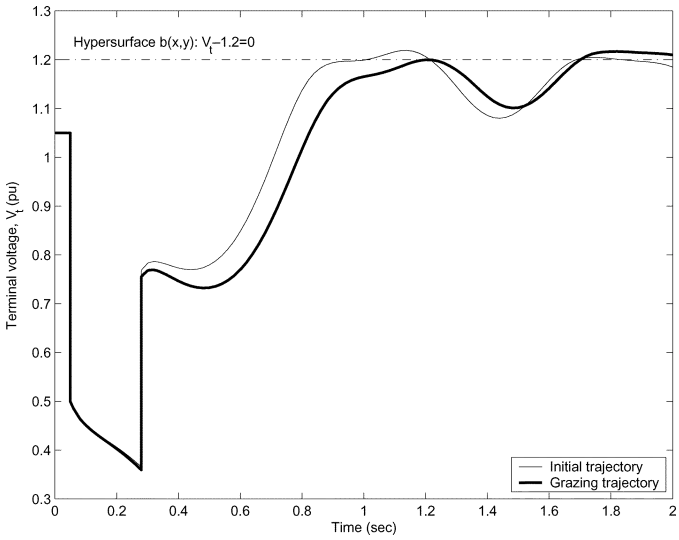

Fig. 7. Terminal voltage V_t, initial and grazing conditions.

(18) not only describes peaks but also troughs and points of inflection. It turns out that for this example, (18) actually has three solutions in close proximity. Accordingly, the Jacobian DF_g is quite ill-conditioned. It was found that if the second derivative terms in (20) were ignored, the shooting method converged but to the wrong solution. This occurred for initial conditions over most of the extended peak. Clearly the directional information provided by the second derivative terms is important in cases such as this, where the encounter between the trajectory and the border is not unimodal.

It is evident from Fig. 8 that this system exhibits quite nonsmooth behavior. In fact, 15 events occur over the initial 2 s transient, primarily $V_{\rm PSS}$ banging on maximum and minimum limits. Discrete events clearly exert a strong influence on system dynamics. However, because the trajectory sensitivities, and hence the Jacobian DF_g, take those events into account, shooting method convergence is unaffected.

Notice in Fig. 7 that enforcing the performance specification at the first peak has a detrimental effect on the second peak. This reflects the fact that the grazing formulation (18) solves for local encounters between the trajectory and the tangent hypersurface. To ensure absolute compliance with the specification, the grazing trajectory should be monitored for later transgressions. If the specification is exceeded elsewhere, the algorithm should be reinitialized at that crossing point.

In this particular example, due to the unusual choice of $E_{fd\max}$ as the free parameter, there is no value that allows both peaks to simultaneously satisfy the specification. However, such compliance could be achieved by freeing a second parameter and coupling together two sets of equations of the form (14)–(17).

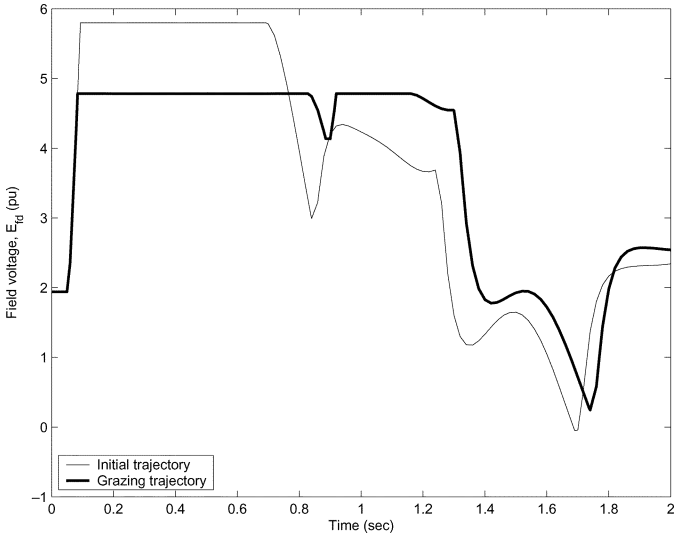

Fig. 8. Generator field voltage E_{fd}, initial and grazing conditions.

IV. TIME-DIFFERENCE EVENT TRIGGERS

Often events are not triggered instantaneously but rather require a condition to be satisfied for a specified time period τ. For example, zone 2 and 3 distance relays do not trip instantaneously but issue a trip signal only after the apparent impedance has remained within the zone characteristic for a preset time. Tangential contact no longer plays a role, so the grazing formulation (14)–(17) is now inappropriate. However, conditions that just induce an event (analogous to grazing) can again be formulated analytically.

A. Mathematical Formulation

Let a system trajectory encounter an enabling condition $b_1(x,y)=0$ at time t_1 and the disabling condition $b_2(x,y)=0$ at time t_2. If the time difference t_2-t_1 is less than the time τ required for triggering, then no event will occur. However, if $t_2-t_1>\tau$, then the event will occur. The pivotal condition corresponds to $t_2-t_1=\tau$. These conditions can be formulated as

$$F_{d1}(x_1,\theta,t_1) := \phi(x_0(\theta),t_1)-x_1=0 \tag{26}$$
$$F_{d2}(x_1,y_1) := g(x_1,y_1)=0 \tag{27}$$
$$F_{d3}(x_2,\theta,t_2) := \phi(x_0(\theta),t_2)-x_2=0 \tag{28}$$
$$F_{d4}(x_2,y_2) := g(x_2,y_2)=0 \tag{29}$$
$$F_{d5}(x_1,y_1) := b_1(x_1,y_1)=0 \tag{30}$$
$$F_{d6}(x_2,y_2) := b_2(x_2,y_2)=0 \tag{31}$$
$$F_{d7}(t_1,t_2) := (t_2-t_1)-\tau=0 \tag{32}$$

where (x_1,y_1) and (x_2,y_2) give the enabling and disabling points, respectively. It takes t_1 and t_2 seconds, respectively, to reach those points from the initial condition $x_0(\theta)$. This set of equations may be written compactly as

$$F_d(x_1,y_1,x_2,y_2,\theta,t_1,t_2)=F_d(z)=0 \tag{33}$$

TABLE III
SHOOTING METHOD CONVERGENCE, TIME-DIFFERENCE PROTECTION TRIGGERING

Iter	Pivotal values		
	ΔP_L at bus 4	t_1 (sec)	t_2 (sec)
0	00.0%	0.27	0.50
1	46.7%	0.22	0.52
2	68.9%	0.29	0.59
3	66.8%	0.29	0.59
4	66.6%	0.29	0.59

where $z = \left[x_1^T\ y_1^T\ x_2^T\ y_2^T\ \theta\ t_1\ t_2\right]^T$ and $F_d : \mathbb{R}^{2n+2m+3} \rightarrow \mathbb{R}^{2n+2m+3}$. Solution of (26)–(32) can be obtained by a shooting method, using an update formula similar to (19). In this case, the Jacobian becomes

$$DF_d = \begin{bmatrix} -I & 0 & 0 & 0 & \Phi|_{t_1}\frac{dx_0}{d\theta} & f|_{t_1} & 0 \\ g_x|_{t_1} & g_y|_{t_1} & 0 & 0 & 0 & 0 & 0 \\ 0 & 0 & -I & 0 & \Phi|_{t_2}\frac{dx_0}{d\theta} & 0 & f|_{t_2} \\ 0 & 0 & g_x|_{t_2} & g_y|_{t_2} & 0 & 0 & 0 \\ b_{1,x}|_{t_1} & b_{1,y}|_{t_1} & 0 & 0 & 0 & 0 & 0 \\ 0 & 0 & b_{2,x}|_{t_2} & b_{2,y}|_{t_2} & 0 & 0 & 0 \\ 0 & 0 & 0 & 0 & 0 & -1 & 1 \end{bmatrix}. \tag{34}$$

B. Initialization of Variables

Iterative solution of (26)–(32) again requires good initial guesses for all variables. The techniques of Section III-C-II can be adapted to provide appropriate values. Again the trajectory induced by parameter θ^0 should be monitored for intersections with the enabling and disabling hypersurfaces.

1) If an intersection with the enabling surface exists, it provides x_1^0, y_1^0, t_1^0. The trajectory should then be continued until the disabling hypersurface is encountered, giving x_2^0, y_2^0, t_2^0. If that encounter does not occur around time $t_1^0 + \tau$, then the latter point should be given by x, y values at $t_2^0 \approx t_1^0 + \tau$.
2) If the trajectory does not intersect the enabling hypersurface at all, then the point where $db_1/dt = 0$ should be identified, as in Section III-C-II. From that point, it is often sufficient to take a time step τ along the trajectory to x_2^0, y_2^0, t_2^0. Other strategies may also be appropriate, depending on the nature of b_1 and b_2. For example, if $b_1 = b_2 = b$, then it may be more appropriate to take a time step $\tau/2$ backward to give x_1^0, y_1^0, t_1^0 and forward to give x_2^0, y_2^0, t_2^0.

C. Example: Protection (Revisited)

The example of Section III-D will again be used, though in this case the instantaneous trip of relay 24 has been replaced by a delayed trip. The impedance trajectory must remain within the circle characteristic for $\tau = 0.3$ s for a trip to occur. Therefore, in this case, the enabling and disabling hypersurfaces are both given by the protection circle characteristic, so that $b_1 = b_2 = b$. Equations (26)–(32) were solved to determine the change in bus 4 load that would just induce a trip under these revised conditions. As indicated in Table III, the shooting method converged in four iterations and found that a 66.6% load increase was required. Fig. 9 shows this pivotal case, along with the original trajectory.

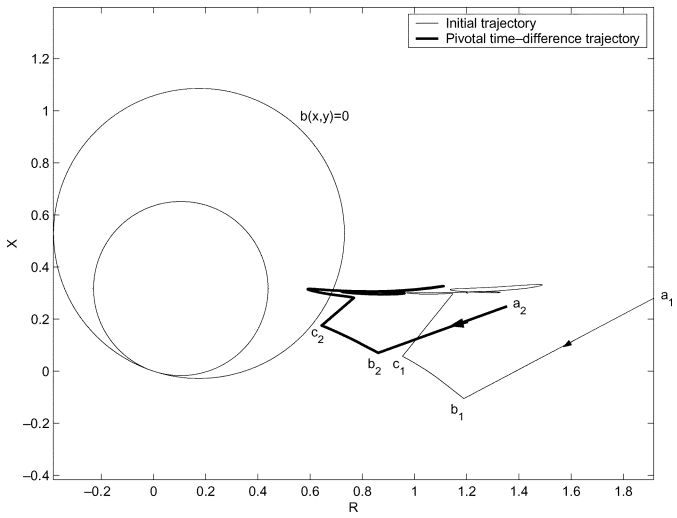

Fig. 9. Impedance trajectories, time-difference event triggering.

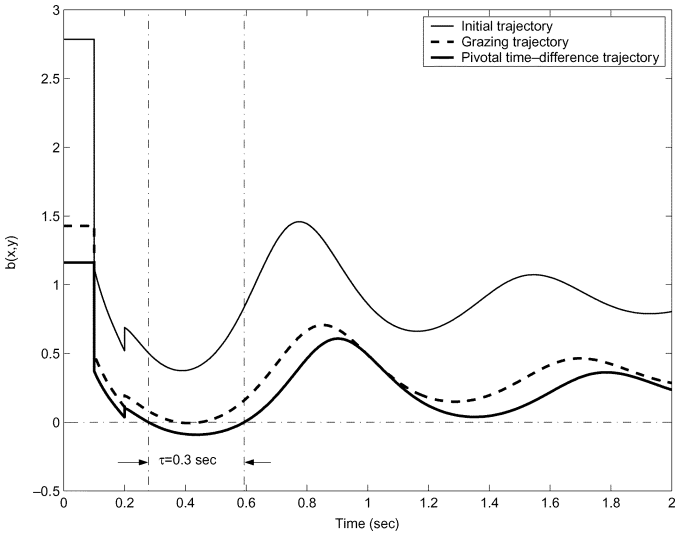

Fig. 10. Evaluation of $b(x, y)$ along trajectories.

Fig. 10 compares time-domain trajectories of $b(x, y)$ for the three cases of interest, viz., nominal load at bus 4, load corresponding to grazing (instantaneous tripping), and the final case when tripping occurred after 0.3 s. Notice that the nominal trajectory does not dip below the $b(x, y) = 0$ threshold, so no tripping is initiated. The grazing trajectory makes tangential contact with the $b(x, y) = 0$ axis, while the time-difference case lies below the axis for exactly the specified $\tau = 0.3$ s.

D. Example: Induction Motor Stalling

Time-difference events can be further illustrated by considering fault-induced induction motor stalling. The simple system of Fig. 11, consisting of a load bus connected to the Thévenin equivalent of the supply system, is sufficient for examining this phenomenon. An induction motor and static var compensator

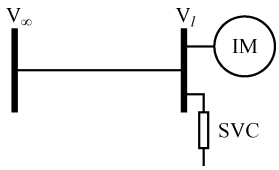

Fig. 11. Induction motor supply system.

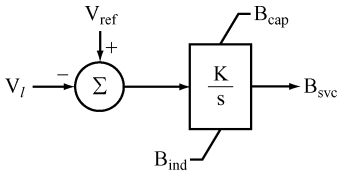

Fig. 12. Static var compensator model.

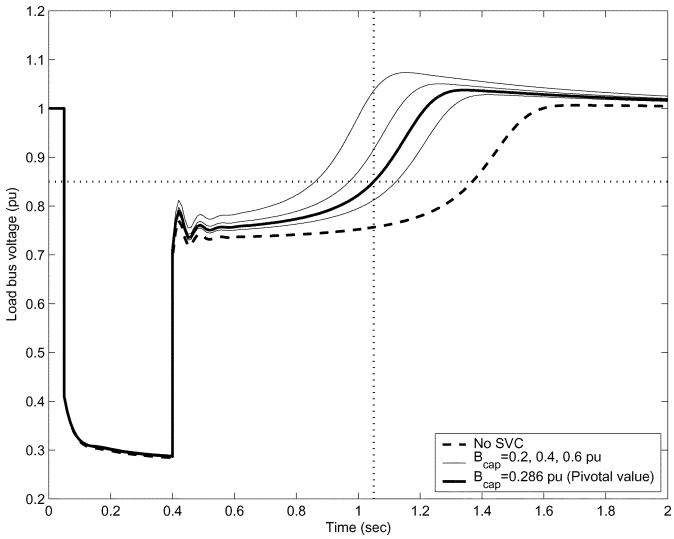

Fig. 13. Voltage response to a fault, various SVC maximum limits.

(SVC) are connected at the load bus. For this example, the induction motor has been represented by a third-order model [31], while the SVC model is shown in Fig. 12.

A fault near the load bus will cause the induction motor slip to increase. If the slip advances too far during the fault, the motor will stall. Even if stalling does not occur, a near-stall condition will prolong the post-fault voltage recovery. This is shown in Fig. 13. Protection is usually set to trip the motor in response to prolonged low-voltage conditions.

An SVC can be used to improve fault recovery by supporting the load bus voltage [32]. The level of support depends upon the SVC's capacitive limit $B_{\rm cap}$, as illustrated in Fig. 13. Support increases with $B_{\rm cap}$, but so does the SVC cost. It is useful to determine the smallest $B_{\rm cap}$ that prevents motor tripping. This fits a time-difference event formulation.

For this example, a fault was applied at the load bus at 0.05 s and cleared at 0.4 s. The motor protection was set to operate if the voltage remained below 0.85 p.u. for longer than 1 s. These specifications have the form of a time-difference event, with fault initiation providing the enabling condition, voltage rising above 0.85 p.u. establishing the disabling condition, and time difference $\tau = 1$ s. In this case though, the fault occurs at a

TABLE IV
SHOOTING METHOD CONVERGENCE, INDUCTION MOTOR TRIPPING

Iter	Pivotal values	
	$B_{\rm cap}$ (pu)	$V_l(1.05)$ (pu)
0	0.000	0.756
1	0.463	0.957
2	0.293	0.854
3	0.286	0.850

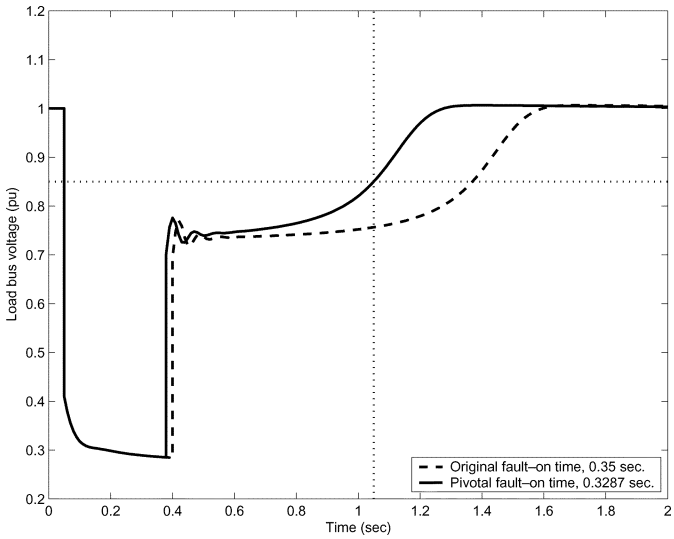

Fig. 14. Voltage response to a fault, various fault-on times.

user-specified time of $t_1 = 0.05$ s, with the system in pre-fault steady state, so x_1, y_1, t_1 are immediately known. Furthermore, (32) can be solved directly to obtain $t_2 = 1.05$ s. The time-difference formulation (26)–(32) reduces to

$$F_{d3}(x_2, \theta) := \phi(x_0(\theta), t_2) - x_2 = 0 \tag{35}$$

$$F_{d4}(x_2, y_2) := g(x_2, y_2) = 0 \tag{36}$$

$$F_{d6}(x_2, y_2) := b_2(x_2, y_2) = 0 \tag{37}$$

where $b_2(x_2, y_2) \equiv V_l(1.05) - 0.85$, and $\theta \equiv B_{\rm cap}$. The shooting method was used to solve (35)–(37), with convergence progress given in Table IV. The pivotal trajectory, corresponding to $B_{\rm cap} = 0.286$ p.u., is shown in Fig. 13. Notice that this voltage trajectory passes through $V_l = 0.85$ p.u. at exactly 1.05 s. Incrementally slower recovery would result in motor tripping.

Rather than installing an SVC at the load bus, it may be more cost effective to reduce the fault-clearing time. To explore this option, the SVC was removed from the system, and the example was reworked accordingly. As shown in Fig. 14, pivotal conditions were achieved by reducing the fault-on time from 0.35 to 0.3287 s. This result was achieved in four iterations and further illustrates the versatility of the analysis approach suggested throughout the paper.

V. CONCLUSIONS

Performance specifications place restrictions on the dynamic behavior of systems. Such specifications dictate regions of parameter space where operation is acceptable. Parameter values on the boundary of those regions result in dynamic behavior that

only just meets specifications.[2] In defining such borderline behavior, two cases must be considered:

1) an encounter with a performance constraint has instantaneous consequences; or
2) a triggering condition must be satisfied for a certain time period.

In the first case, bounding (parameter space) conditions give rise to grazing phenomena (in state space), where the system trajectory tangentially encounters (grazes) the performance constraint. The second case replaces tangential contact by a requirement that the time difference between enabling and disabling conditions exactly matches a specified trigger time.

Both sets of pivotal conditions can be formulated as boundary value problems. Newton's method robustly solves the corresponding nonlinear algebraic equations. Each iteration requires numerical integration of the system trajectory, so the solution process has the form of a shooting method. The associated Jacobian incorporates trajectory sensitivities, which can be efficiently computed along with the trajectory. The shooting method is therefore practical for arbitrarily large power systems.

Applications of this approach to assessing dynamic performance are extensive. The paper considers a diverse array of examples, drawn from distance protection operation (both instantaneous and delayed), transient over-voltages, and induction motor stalling.

REFERENCES

[1] "Final Report on the August 14, 2003 Blackout in the United States and Canada: Causes and Recommendations," U.S.-Canada Power System Outage Task Force, 2004.

[2] J. Blackburn, *Protective Relaying Principles and Applications*, 2nd ed. New York: Marcel Dekker, 1998.

[3] C. Singh and I. Hiskens, "Direct assessment of protection operation and nonviable transients," *IEEE Trans. Power Syst.*, vol. 16, no. 3, pp. 427–434, Aug. 2001.

[4] J. Stoer and R. Bulirsch, *Introduction to Numerical Analysis*, 2nd ed. New York: Springer-Verlag, 1993.

[5] M. Fredriksson and A. Nordmark, "Bifurcations caused by grazing incidence in many degrees of freedom impact oscillators," *Proc. R. Soc. London A*, vol. 453, no. 1961, pp. 1261–1276, 1997.

[6] M. di Bernardo, C. Budd, and A. Champneys, "Grazing and border-collision in piecewise-smooth systems: A unified analytical framework," *Phys. Rev. Lett.*, vol. 86, no. 12, pp. 2553–2556, Mar. 2001.

[7] V. Donde and I. Hiskens, "Shooting methods for locating grazing phenomena in hybrid systems," *Int. J. Bifurcation Chaos*, to be published.

[8] A. van der Schaft and H. Schumacher, *An Introduction to Hybrid Dynamical Systems*. London, U.K.: Springer-Verlag, 2000.

[9] D. Liberzon, *Switching in Systems and Control*. Boston, MA: Birkhauser, 2003.

[10] M. di Bernardo, H. Chung, and C. Tse, "Guest editorial: Special issue on switching and systems," *IEEE Trans. Circuits Syst. I: Fundam. Theory Appl.*, vol. 50, no. 8, pp. 973–974, Aug. 2003.

[11] R. David and H. Alla, *Petri Nets and Grafecet*. Englewood Cliffs, NJ: Prentice-Hall, 1992.

[12] I. Hiskens, "Power system modeling for inverse problems," *IEEE Trans. Circuits Syst. I: Reg. Papers*, vol. 51, no. 3, pp. 539–551, Mar. 2004.

[13] I. Hiskens and M. Pai, "Trajectory sensitivity analysis of hybrid systems," *IEEE Trans. Circuits Syst. I: Fundam. Theory Appl.*, vol. 47, no. 2, pp. 204–220, Feb. 2000.

[14] L. Perez, A. Flechsig, and V. Venkatasubramanian, "Modeling the protective system for power system dynamic analysis," *IEEE Trans. Power Syst.*, vol. 9, no. 4, pp. 1963–1973, Nov. 1994.

[15] I. Hiskens and P. Sokolowski, "Systematic modeling and symbolically assisted simulation of power systems," *IEEE Trans. Power Syst.*, vol. 16, no. 2, pp. 229–234, May 2001.

[16] P. Frank, *Introduction to System Sensitivity Theory*. New York: Academic, 1978.

[17] W. Feehery, J. Tolsma, and P. Barton, "Efficient sensitivity analysis of large-scale differential-algebraic systems," *Appl. Num. Math.*, vol. 25, pp. 41–54, 1997.

[18] S. Li, L. Petzold, and W. Zhu, "Sensitivity analysis of differential-algebraic equations: A comparison of methods on a special problem," *Appl. Num. Math.*, vol. 32, no. 8, pp. 161–174, 2000.

[19] H. Dankowicz, P. Piiroinen, and A. Nordmark, "Low-velocity impacts of quasi-periodic oscillations," *Chaos, Solitons, Fractals*, vol. 14, pp. 241–255, 2002.

[20] W. Chin, E. Ott, H. Nusse, and C. Grebogi, "Universal behavior of impact oscillators near grazing incidence," *Phys. Lett. A*, vol. 201, no. 2–3, pp. 197–204, Mar. 1995.

[21] H. Nusse, E. Ott, and J. Yorke, "Border-collision bifurcations: An explanation for observed bifurcation phenomena," *Phys. Rev. E*, vol. 49, no. 2, pp. 1073–1077, Feb. 1994.

[22] G. Yuan, S. Banerjee, E. Ott, and J. Yorke, "Border-collision bifurcations in the buck converter," *IEEE Trans. Circuits Syst. I*, vol. 45, no. 7, pp. 707–715, Jul. 1998.

[23] M. di Bernardo, M. Feigen, S. Hogan, and M. Homer, "Local analysis of C-bifurcations in n-dimensional piecewise-smooth dynamical systems," *Chaos, Solitons, Fractals*, vol. 10, no. 11, pp. 1881–1908, 1999.

[24] R. Rajaraman, I. Dobson, and S. Jalali, "Nonlinear dynamics and switching time bifurcations of a thyristor controlled reactor circuit," *IEEE Trans. Circuits Syst. I*, vol. 43, no. 12, pp. 1001–1006, Dec. 1996.

[25] S. Jalali, I. Dobson, R. Lasseter, and G. Venkataramanan, "Switching time bifurcations in a thyristor controlled reactor," *IEEE Trans. Circuits Syst. I*, vol. 43, no. 3, pp. 209–218, Mar. 1996.

[26] N. Narasimhamurthi and M. Musavi, "A generalized energy function for transient stability analysis of power systems," *IEEE Trans. Circuits Syst.*, vol. 31, no. 7, pp. 637–645, Jul. 1984.

[27] V. Donde, "Inverse problems in hybrid systems with application to power systems," Ph.D. dissertation, Univ. Illinois at Urbana-Champaign, 2004.

[28] P. Sauer and M. Pai, *Power System Dynamics and Stability*. Upper Saddle River, NJ: Prentice-Hall, 1998.

[29] *IEEE Recommended Practice for Excitation System Models for Power System Stability Studies*, IEEE Std 421.5–1992, 1992.

[30] G. Goodwin, S. Graebe, and M. Salgado, *Control System Design*. Upper Saddle River, New Jersey: Prentice-Hall, 2001.

[31] P. Kundur, *Power System Stability and Control*. New York: McGraw-Hill, 1994, EPRI Power System Engineering Series.

[32] A. Hammad and M. El-Sadek, "Prevention of transient voltage instabilities due to induction motor loads by static var compensators," *IEEE Trans. Power Syst.*, vol. 4, no. 3, pp. 1182–1190, Aug. 1989.

[2]Note the important but subtle distinction between boundaries in *parameter space* and performance specifications (boundaries) in *state space*.

Vaibhav Donde (S'01–M'04) received the B.E. degree from Veermata Jijabai Technological Institute, Mumbai, India, in 1998 and the M.S. and Ph.D. degrees from the University of Illinois at Urbana-Champaign in 2000 and 2004, respectively, all in electrical engineering.

He was with Tata Consulting Engineers, Mumbai, from 1998 to 1999. He is currently a Postdoctoral Research Fellow at Lawrence Berkeley National Laboratory, Berkeley, CA. His technical interests include power systems analysis and computational aspects, hybrid dynamic systems, and nonlinear control.

Ian A. Hiskens (S'77–M'80–SM'96) received the B.Eng. degree in electrical engineering and the B.App.Sc. degree in mathematics from the Capricornia Institute of Advanced Education, Rockhampton, Australia, in 1980 and 1983, respectively, and the Ph.D. degree from the University of Newcastle, Newcastle, Australia, in 1991.

He is a Professor of electrical and computer engineering at the University of Wisconsin-Madison. He has held prior appointments with the Queensland Electricity Supply Industry, Australia, from 1980 to 1992, the University of Newcastle, from 1992 to 1999, and the University of Illinois at Urbana-Champaign, from 1999 to 2002. His major research interests lie in the area of power system analysis, in particular system dynamics, security, and numerical techniques. Other research interests include nonlinear and hybrid systems and control.